INTERNATIONAL ATOMIC ENERGY AGENCY
UNITED NATIONS EDUCATIONAL, SCIENTIFIC AND CULTURAL ORGANIZATION

INTERNATIONAL CENTRE FOR THEORETICAL PHYSICS
34100 TRIESTE (ITALY) - P.O.B. 586 - MIRAMARE - STRADA COSTIERA 11 - TELEPHONES: 224281/2/3/4/5/6
CABLE: CENTRATOM - TELEX 460392-1

SMR/113 - 5

AUTUMN COLLEGE

ON

THE TROPOSPHERE, STRATOSPHERE AND MESOSPHERE

10 September - 19 October 1984

EXPERIMENTS WITH ROTATING FLUIDS

R. HIDE

Geophysical Fluid Dynamics Laboratory
Meteorological Office (21)
Bracknell
Berkshire RG12 2SZ
U.K.

(*From the* QUARTERLY JOURNAL OF THE ROYAL METEOROLOGICAL SOCIETY, Vol. 103, No. 435, January 1977)

QUARTERLY JOURNAL
OF THE
ROYAL METEOROLOGICAL SOCIETY

Vol. 103 JANUARY 1977 No. 435

Quart. J. R. Met. Soc. (1977), **103**, pp. 1–28

551.511.32: 532.5

Experiments with rotating fluids

By R. HIDE

(Presidential Address: 21 April 1976)

1. INTRODUCTION

At the turn of the present century an eminent physicist expressed the firm opinion that perfectly accurate weather forecasts would be available by the year 1950. He did not consider it necessary to explain how this development would come about, presumably because he shared the view of many of his contemporaries that further work on macroscopic systems satisfying the laws of classical physics would be a matter of mere routine, requiring no more than the diligent efforts of a sufficient number of dedicated but not necessarily inspired investigators. This attitude led to the neglect of important areas of physics, so it is hardly surprising to find today, with three-quarters of the twentieth century gone, that insufficient knowledge of various hydrodynamical processes still constitutes a major difficulty not only in meteorology, but also in oceanography and other geophysical sciences.

In this address I propose to discuss one area of 'geophysical fluid dynamics' in which I have been engaged with various colleagues over a number of years, namely the study of rapidly-rotating fluids. Our work has, by choice, centred largely on laboratory investigations, but mathematical studies are found necessary in the formulation of crucial experiments and the interpretation of their results. Numerical studies employing high-speed electronic computers are becoming increasingly important in our work, but in spite of their many attractions computers are still comparatively very expensive to use and to date they have been employed successfully only in detailed investigations of the less complex types of flow encountered in laboratory work.

It is unnecessary to apologize for discussing simple systems that can be realized in the laboratory, and asserting their relevance to the science of atmospheres and oceans, since the essence of basic science, upon which all applied science depends, is the obtaining of general results concerning well-defined problems, not limited results concerning only vaguely-defined problems. A critical review of recent progress made with the study of rotating fluids would, however, take much more than an hour to present and interest only specialists in dynamics, so in preparing this address to a wider audience I considered it preferable to take a didactic approach, with a view to showing that a few theorems and other basic theoretical results (see section 2) suffice to provide considerable insight into the behaviour of a variety of mechanically and thermally-driven systems, such as those few selected for discussion under the various section headings of this paper, namely flows due to oscillatory mechanical forcing (section 3), steady source-sink flows (section 4) and thermal convection due to an impressed horizontal temperature gradient (section 5).

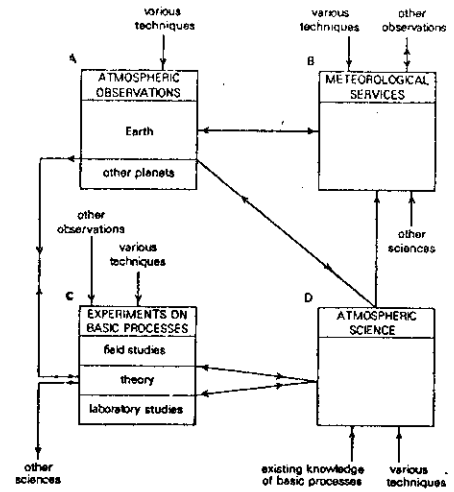

Figure 1. An attempt to illustrate the relationship between atmospheric science, applied meteorology and research on basic processes (see text).

But with an audience consisting mainly of meteorologists it is necessary before going into details to consider how the study of basic processes bears on atmospheric science generally and is thus able to contribute, at least potentially, to practical meteorology. A rough and inevitably over-simplified attempt to portray the complex relationships involved is illustrated in Fig. 1. Box B at the top right-hand corner represents meteorological services, the provision of which to the public and to other scientists involves the application of meteorological knowledge to a wide range of practical problems. Box A at the top left represents the routine acquisition and analysis of (a) observations of the earth's atmosphere, which are made largely to meet the needs of meteorological services, and (b) observations of the atmospheres of other planets, the collection of which was initiated over a century ago by amateur astronomers but is now undertaken in collaboration with observatories staffed with professional workers. Box D at the bottom right represents the development of a body of knowledge known as atmospheric science, which comprises the systematic description or interpretation of atmospheric phenomena, as revealed by observations, in terms of basic physical* and chemical processes. Box C at the bottom left represents research on basic processes, involving experimental field or laboratory (including numerical) investigations rendered crucial through close contact with appropriate theory. Box C would not, of course, be needed if the textbooks of physics and chemistry contained all the information and ideas required for the purposes of atmospheric science.

Theory without contact with experiments is an uncertain and often pointless venture and the direct link AD between observations and atmospheric science is weaker than the indirect link through the intermediary of experiments on basic processes (box C). The link AC involves speculation, but when this is followed by well-formulated theories fully tested

* Here 'physics' is taken in the generally accepted sense and not as implied by unfortunate jargon employed by some dynamical meteorologists when, in their descriptions of numerical models of large-scale motions in the atmosphere, they use the term to refer to processes not explicitly represented in the models, such as small-scale dynamical processes, radiation, clouds, etc.

by crucial field or laboratory studies, true scientific advances are made and, what is equally important, practical meteorologists are presented with opportunities to improve the services they are asked to provide. Laboratory experiments with rotating fluids fall within the middle and lower subdivisions of box C. They are comparatively cheap to carry out and could easily be pursued without reference to observational studies in meteorology, oceanography, etc. Indeed, in retrospect one can see that some of the most relevant work has been motivated not by the direct demands of atmospheric science and practical meteorology but by sheer scientific curiosity. This state of affairs is by no means unusual when seen in the context of the development of ideas in other fields of science, and a few leading meteorologists have been quick to appreciate and exploit the results of laboratory work. Others, however, including several prominent workers, have evidently misunderstood the role of laboratory experiments by supposing, unjustifiably in my opinion, that the objective of the laboratory work should be the construction of purblind models merely for the purpose of improving the direct link AB or AD in Fig. 1. Much has been said by these critics about the differences between laboratory systems and the real atmosphere, and it is true that without a method of simulating a radially-symmetric gravitational field it will never be possible to construct a perfect laboratory 'model' in the engineering sense. But surely the very essence of the problem of understanding the circulation of the atmosphere is not just to create a replica but to study a hierarchy of related but different systems; it is a matter for investigation whether or not the shape of the boundary, for example, is important, not for *a priori* assessment (see e.g. Hide 1969, Monin 1972).

2. Some useful theoretical results

(i) *Equations of motion of an incompressible Boussinesq fluid.* When dealing with most geophysical and laboratory systems it is sufficient to consider the behaviour of a fluid in which (a) the velocities are so small in comparison with the speed of sound that the assumption of incompressibility is valid, and (b) the accelerations are so small in comparison with gravity that the Boussinesq approximation (which takes density variations into account in the buoyancy term in the equations of motion but not in the other terms) can be used. When referred to a system that rotates with steady angular velocity Ω relative to an inertial frame, the equations of continuity and momentum of such a fluid of uniform kinematic viscosity ν and variable density $\bar{\rho}(1+\theta)$, where $\bar{\rho}$ is the mean density and $\theta \ll 1$, are:

$$\nabla.\mathbf{u} = 0 \qquad (2.1)$$

and

$$\partial\mathbf{u}/\partial t + (2\boldsymbol{\Omega}+\boldsymbol{\xi})\times\mathbf{u} = -\nabla(P+\tfrac{1}{2}\mathbf{u}.\mathbf{u}) + \mathbf{g}\theta + \nu\nabla^2\mathbf{u}. \qquad (2.2)$$

Here $\mathbf{u}$ is the Eulerian flow velocity relative to the rotating frame and $\boldsymbol{\xi} \equiv \nabla\times\mathbf{u}$ is the corresponding vorticity vector, t denotes time, $\mathbf{g}$ the acceleration due to gravity plus centrifugal effects, and $\bar{\rho}\nabla P$ is equal to the pressure gradient minus $\mathbf{g}\bar{\rho}$.

Variations in density may be due to changes in temperature, salinity, etc., and in general θ satisfies an equation of the form

$$\partial\theta/\partial t + (\mathbf{u}.\nabla)\theta = \chi\nabla^2\theta + \bar{Q} \qquad (2.3)$$

where χ is a diffusion coefficient and $\bar{Q}$ represents effects due to internal sources; in the case of thermally-driven flows $\bar{Q}$ is proportional to the rate of internal heating per unit mass. When the r.h.s. of Eq. (2.3) vanishes we have

$$D\theta/Dt = 0 \qquad (2.4)$$

(where $D/Dt \equiv \partial/\partial t + \mathbf{u}.\nabla$), implying that the value of θ of an individual fluid element then remains constant throughout the motion.

(ii) *Energetics.* An energy equation follows from Eq. (2.2) when that equation is multiplied scalarly by $\mathbf{u}$ (noting that the second term on the l.h.s. vanishes because it represents a force acting at right-angles to $\mathbf{u}$ and therefore does no work); whence

$$\partial(\tfrac{1}{2}\mathbf{u}.\mathbf{u})/\partial t = -\nu\boldsymbol{\xi}.\boldsymbol{\xi} + \mathbf{u}.g\theta - \nabla.[\tfrac{1}{2}\mathbf{u}(\mathbf{u}.\mathbf{u}) + \mathbf{u}P + \nu(\boldsymbol{\xi}\times\mathbf{u})]. \quad . \quad (2.5)$$

When integrated over a given volume, the l.h.s. represents the rate of change of total kinetic energy and the first term on the r.h.s. (which is essentially negative) represents viscous dissipation of kinetic energy. The second term on the r.h.s. represents the rate at which buoyancy forces convert into kinetic energy the potential energy of gravity acting on the density field. It can in general take either sign, depending on the sign of the average correlation between density variations, proportional to θ, and the vertical component of velocity, proportional to $\mathbf{u}.\mathbf{g}$, but in the case of thermally-driven motions (see e.g. Dutton and Johnson 1967; Van Mieghem 1973; also section 5 below) this buoyancy term is essentially positive when integrated over the whole system.

The last term on the r.h.s. represents mechanical forcing. When integrated, this term can be converted into a surface integral comprising three contributions representing, respectively, the advection of kinetic energy over the surface, the rate of working of normal pressure forces, and the rate of working of tangential viscous forces. Each contribution can take either sign but their sum when integrated over the whole system must be positive in cases of mechanically-driven flows (see sections 3 and 4).

(iii) *Vorticity equation; Jeffreys' theorem and Ertel's theorem.* Equation (2.2) expresses the balance of *forces* acting on individual fluid elements. The corresponding *torque* balance is expressed by the vorticity equation obtained by taking the curl of Eq. (2.2); thus

$$\partial\boldsymbol{\xi}/\partial t + (\mathbf{u}.\nabla)\boldsymbol{\xi} - [(2\boldsymbol{\Omega}+\boldsymbol{\xi}).\nabla]\mathbf{u} = -\mathbf{g}\times\nabla\theta + \nu\nabla^2\boldsymbol{\xi}. \quad . \quad (2.6)$$

This equation leads directly to a general result which goes under several names but is conveniently referred to as 'Jeffreys' theorem' and concerns the conditions under which hydrostatic equilibrium obtains, defined as $\mathbf{u} = 0$ everywhere. By Eq. (2.6), $\mathbf{u} = 0$ when $\mathbf{g}\times\nabla\theta = 0$, implying that *hydrostatic equilibrium is impossible if density variations occur on level surfaces.* Jeffreys' theorem is a direct corollary of Bjerknes' well-known circulation theorem (see Eliassen and Kleinschmidt 1957); it provides the most direct demonstration that the atmosphere *must* circulate under the influence of solar heating, which maintains a generally north–south density gradient on level surfaces.

We now introduce a quantity known as 'potential vorticity' and defined as

$$(2\boldsymbol{\Omega}+\boldsymbol{\xi}).\nabla\Lambda, \quad . \quad . \quad . \quad . \quad (2.7)$$

where Λ is any quantity satisfying

$$D\Lambda/Dt = 0 \quad . \quad . \quad . \quad . \quad (2.8)$$

(cf. Eq. (2.4)). By Eq. (2.6)

$$D[(2\boldsymbol{\Omega}+\boldsymbol{\xi}).\nabla\Lambda]/Dt = -(\mathbf{g}\times\nabla\theta).\nabla\Lambda + \nu\nabla\Lambda.\nabla^2\boldsymbol{\xi} \quad . \quad (2.9)$$

and therefore

$$D[(2\boldsymbol{\Omega}+\boldsymbol{\xi}).\nabla\Lambda]/Dt = 0 \quad . \quad . \quad . \quad (2.10)$$

when the fluid is homogeneous ($\nabla\theta = 0$) *and inviscid.* This is Ertel's particularly useful theorem (see e.g. Charney 1973; Eliassen and Kleinschmidt 1957; Greenspan 1968; Krauss 1973; Pedlosky 1971) for an incompressible Boussinesq fluid.

(iv) *Two-dimensional flows: Taylor's theorem and Fjørtoft's theorem.* When the fluid is homogeneous ($\nabla\theta = 0$) and, in virtue of the boundary conditions, $\mathbf{u} = (u, v, w)$ is independent of the coordinate z parallel to the rotation axis, the relative vorticity has no (transverse) components in the (x, y) directions (i.e. $\boldsymbol{\xi} = (\xi, \eta, \zeta) = (0, 0, \zeta)$) and the axial component of $\boldsymbol{\xi}$ satisfies

$$\partial\zeta/\partial t + u\,\partial\zeta/\partial x + v\,\partial\zeta/\partial y = \nu(\partial^2\zeta/\partial x^2 + \partial^2\zeta/\partial y^2). \quad . \quad (2.11)$$

The angular velocity vector $\boldsymbol{\Omega}$ does not appear in this equation, implying that *if* $\mathbf{u}$ *is independent of* z *and the boundary conditions on* $\mathbf{u}$ *are independent of* $\boldsymbol{\Omega}$, *then* $\mathbf{u}$ *is independent of* $\boldsymbol{\Omega}$ (see Taylor 1917). The pressure field, on the other hand, is *not* unaffected by rotation; by Eq. (2.2) P exceeds its value for $\boldsymbol{\Omega} = 0$ by an amount $\hat{P}$ where

$$\nabla\hat{P} + 2\boldsymbol{\Omega}\times\mathbf{u} = 0. \quad . \quad . \quad . \quad . \quad (2.12),$$

Laboratory experiments bearing on this theorem have been carried out by Taylor (1917) who demonstrated the existence of the $\boldsymbol{\Omega}$-dependent part of the pressure field by determining the trajectories of moving objects, and by Hide (1968), who investigated flows due to various distributions of sources and sinks and demonstrated that $\mathbf{u}$ is independent of $\boldsymbol{\Omega}$ when sources and sinks of the monopole (but not dipole) type are absent but not when they are present (see section 4).

The vanishing of the r.h.s. of Eq. (2.11) when viscous effects are negligible shows that in two-dimensional flow of an inviscid homogeneous fluid the vorticity remains constant throughout the motion (cf. Eq. (2.23) below), so that the total enstrophy (per unit length in the z-direction)

$$\mathscr{E} \equiv \iint\zeta^2\,dxdy, \quad . \quad . \quad . \quad (2.13)$$

where the integral is taken over the whole system, remains fixed (i.e. $d\mathscr{E}/dt = 0$). This result represents a powerful constraint on non-linear interactions between different scales of motion, for in order to conserve both total enstrophy and total kinetic energy (per unit length in the z-direction)

$$\mathscr{K} \equiv \iint\tfrac{1}{2}\bar{\rho}(u^2+v^2)\,dxdy \quad . \quad . \quad . \quad (2.14)$$

(cf. Eq. (2.5)), *the transfer of energy from one scale to a smaller (larger) scale must be accompanied by the simultaneous transfer to a larger (smaller) scale.* Such behaviour of two-dimensional systems, as expressed by this 'anti-cascade' theorem of Fjørtoft and others (Fjørtoft 1953; for additional references see Charney 1973 and Lilly 1973) contrasts strongly with isotropic homogeneous three-dimensional turbulence, where the energy cascade from larger to smaller scales involves a rapid increase in enstrophy, associated with the three-dimensional stretching and twisting terms in the vorticity equation. Whereas the energy spectrum of three-dimensional turbulence follows Kolmogoroff's celebrated (wavenumber)$^{-\frac{5}{3}}$ (energy-dissipation rate)$^{\frac{2}{3}}$ law, that of two-dimensional turbulence satisfies a (wavenumber)$^{-3}$(enstrophy-dissipation rate)$^{\frac{2}{3}}$ law.

(v) *Geostrophic flow; thermal wind equation and Proudman's theorem.* Geostrophic flow occurs in regions where the relative acceleration term $D\mathbf{u}/Dt (= \partial\mathbf{u}/\partial t + \boldsymbol{\xi}\times\mathbf{u} + \nabla(\frac{1}{2}\mathbf{u}.\mathbf{u}))$ in Eq. (2.2) and the viscous term $\nu\nabla^2\mathbf{u}$ can be neglected in comparison with the Coriolis term $2\boldsymbol{\Omega}\times\mathbf{u}$. The Coriolis force then balances the non-hydrostatic component of the pressure force exactly, so that

$$2\boldsymbol{\Omega}\times\mathbf{u} = -\nabla P + g\theta. \quad . \quad . \quad . \quad (2.15)$$

This equation is mathematically degenerate, being of lower order than the complete equation of motion and consequently incapable of solution under *all* the necessary boundary conditions and initial conditions, and it follows that *regions of highly ageostrophic flow (occurring not only on the boundaries of the system but also in the localized regions of the main body of fluid) are necessary concomitants of geostrophic motion.* The geostrophic equation nevertheless expresses with good accuracy various important properties that slow, steady hydrodynamical

motions in a rapidly-rotating fluid must possess nearly everywhere, and when judiciously applied the equation usually indicates the nature and location of essentially ageostrophic features.

A rapidly rotating fluid can be defined as one for which the Rossby number

$$\varepsilon \equiv \langle D\mathbf{u}/Dt \rangle / \langle 2\boldsymbol{\Omega} \times \mathbf{u} \rangle \quad . \quad . \quad . \quad (2.16)$$

and the Ekman number

$$E \equiv \langle \nu \nabla^2 \mathbf{u} \rangle / \langle 2\boldsymbol{\Omega} \times \mathbf{u} \rangle \quad . \quad . \quad . \quad (2.17)$$

are both very much less than unity, the symbol $< >$ meaning the root mean square value taken over the whole volume occupied by the fluid, so that $\varepsilon = U/L\Omega$ and $E = \nu/L^2\Omega$ if U is a typical relative flow speed and L a characteristic length scale. From a mathematical point of view, geostrophic flow occurs in the limit when $\varepsilon \to 0$ and $E \to 0$. The vorticity equation (2.6) then simplifies to

$$(2\boldsymbol{\Omega}.\nabla)\mathbf{u} = \mathbf{g} \times \nabla\theta \quad . \quad . \quad . \quad (2.18)$$

expressing a balance between the gyroscopic torque and the gravitational torque.

When $\nabla\theta = 0$ Eq. (2.18) reduces to

$$2\Omega\, \partial u/\partial z = 0, \quad . \quad . \quad . \quad (2.19)$$

a result first proved by Proudman (1916) and later by others and which goes under various names (e.g. Proudman's theorem, Proudman-Taylor theorem, Taylor-Proudman theorem). In words, Proudman's 'two-dimensional' theorem states that *geostrophic motion of a homogeneous fluid will be the same in all planes perpendicular to the axis of rotation*. This fundamental result underlies the interpretation of a very wide range of phenomena in mechanically-driven flows (see sections 3 and 4 below).

Suppose that (U, V, W) are the (X, Y, Z) components of $\mathbf{u}$, where Z is the downward vertical coordinate, so that in these coordinates $\mathbf{g} = (0, 0, g)$, W is the corresponding vertical component of motion, and (U, V) are the horizontal components. When $\nabla\theta \neq 0$ we have, by Eq. (2.18),

$$(2\boldsymbol{\Omega}.\nabla)(U, V, W) = g(-\partial\theta/\partial Y, \quad \partial\theta/\partial X, \quad 0). \quad . \quad (2.20)$$

In cases when the horizontal component of $\boldsymbol{\Omega}$ is negligible, the first two components of Eq. (2.20) give the familiar thermal wind equation, which expresses the relationship between the vertical rate of change of horizontal geostrophic motion and the horizontal density gradient. It may be shown (Hide 1971) by combining Eq. (2.20) with Eq. (2.4) and setting $\partial\theta/\partial t = 0$ that under steady isentropic conditions

$$(2\boldsymbol{\Omega}.\nabla)(V/U) = -g\frac{W\partial\theta/\partial Z}{U^2+V^2} \quad , \quad . \quad . \quad (2.21)$$

implying that even when, as a result of strong density inhomogeneities, the *speed* of horizontal flow varies rapidly with respect to the axial coordinate z, the corresponding rate of change of the *direction* of horizontal flow may be quite slow and even vanish altogether when $W\partial\theta/\partial Z = 0$.

(vi) *Quasi-geostrophic flow of an inviscid fluid.* Quasi-geostrophic flow occurs when $E \ll 1$ and $\varepsilon \ll 1$, and if $E \ll \varepsilon$ the dominant ageostrophic contributions in the equations of quasi-geostrophic motion are provided by advective effects, not viscosity. Then

$$\partial\mathbf{u}/\partial t + (\mathbf{u}_1.\nabla_1)\mathbf{u} + 2\boldsymbol{\Omega} \times \mathbf{u} = -\nabla P + \mathbf{g}\theta \quad . \quad . \quad (2.22)$$

where $\mathbf{u}_1.\nabla_1 \equiv u\partial/\partial x + v\partial/\partial y$, and the corresponding equation for ζ is

$$\partial\zeta/\partial t + (\mathbf{u}_1.\nabla_1)\zeta \doteq 2\Omega\, \partial w/\partial z - (\mathbf{g} \times \nabla\theta)_z \quad . \quad . \quad (2.23)$$

(see Eqs. (2.2), (2.6), (2.11), (2.16) and (2.17)). Equation (2.23) shows that *in quasi-geostrophic motion of a homogeneous (i.e. $(\mathbf{g} \times \nabla\theta)_z = 0$) incompressible fluid, changes in the relative vorticity of a moving fluid element are brought about largely by axial stretching*, as represented by the term $2\Omega\, \partial w/\partial z$ on the right-hand side.

Suppose for the moment that the buoyancy term can be neglected and that the fluid is bounded by rigid end-walls in $z = z_l(x, y)$ and $z = z_u(x, y)$ where $z_u > z_l$. When effects due to viscous boundary layers are negligible (see section 4), the term $2\Omega\, \partial w/\partial z$ equals $2\Omega\mathbf{u}_1.\nabla_1 \ln(z_u - z_l)$ (to sufficient accuracy) and the equation (2.23) reduces to an expression for the conservation of potential vorticity $(2\Omega + \zeta)/(z_u - z_l)$, namely

$$\{\partial/\partial t + \mathbf{u}_1.\nabla_1\}\{(2\Omega + \zeta)/(z_u - z_l)\} = 0. \quad . \quad . \quad (2.24)$$

(Equation (2.24) follows directly from Ertel's potential vorticity theorem given by Eq. (2.10) when $\mathbf{u}.\nabla$ is approximated by its transverse part $\mathbf{u}_1.\nabla_1$ and $\Lambda = (z - z_l)/(z_u - z_l)$ or $\Lambda = (z_u - z)/(z_u - z_l)$.)

If θ satisfies Eq. (2.4) we can set $\Lambda = \theta$ (cf. Eq. (2.8)) in Eq. (2.9), and if we further assume that $\nu = 0$ the r.h.s. vanishes, giving

$$D[(2\boldsymbol{\Omega} + \boldsymbol{\xi}).\nabla\theta]/Dt = 0. \quad . \quad . \quad . \quad (2.25)$$

In the geostrophic limit, this potential vorticity equation for a non-homogeneous fluid has no general form analogous to Eq. (2.24), but for a shallow system, such as the earth's atmosphere (see e.g. Charney 1973; Obukhov 1974; Pedlosky 1971; Phillips 1963), in which $\varepsilon \ll 1$ (but $> E$), $\theta = \theta_0(Z) + \delta\theta$ with $\delta\theta \ll \theta_0$, $P = P_0(Z) + \delta P$ with $\delta P \ll P_0$ and f is the vertical component of $2\boldsymbol{\Omega}$, so that by Eq. (2.15)

$$(\xi)_Z = -f^{-1}(\partial^2/\partial X^2 + \partial^2/\partial Y^2)\delta P \text{ and } \delta\theta = g^{-1}\partial(\delta P)/\partial Z, \quad . \quad (2.26)$$

Eq. (2.25) reduces to

$$\left(\frac{\partial}{\partial t} + U\frac{\partial}{\partial X} + V\frac{\partial}{\partial Y}\right)\left\{\left(\frac{\partial\theta_0}{\partial Z}\right)\left[f + f\left(\frac{\partial^2}{\partial X^2} + \frac{\partial^2}{\partial Y^2} + \frac{f^2\partial^2/\partial Z^2}{g\partial\theta_0/\partial Z}\right)\right]\delta P\right\} = 0. \quad (2.27)$$

Equation (2.27) is of central importance in a wide range of theoretical investigations in dynamical meteorology and oceanography, including the study of 'geostrophic turbulence' (see section 5), where the constraints on potential vorticity represented by Eq. (2.27) (or (2.24)) place severe restrictions on the types of non-linear interactions that are possible. This results in behaviour (see e.g. Charney 1973; Lilly 1973; Rhines 1976) which is analogous in some respects to that of two-dimensional turbulence in a homogeneous fluid (see e.g. Eqs. (2.12) and (2.13) above and Figs. 10 and 11 below).

3. Flows due to oscillatory mechanical forcing

A fluid differs in an essential way from a solid in its inability in the absence of rotation (and of buoyancy forces due to the action of gravity on stable density stratification or magnetohydrodynamic effects) to resist shearing stresses and thereby support shear waves (see e.g. Lighthill 1966). When the fluid rotates relative to an inertial frame the constraints imposed on the system by angular momentum requirements are such as to endow the fluid with pseudo-elastic properties, and a brief account of the so-called 'elastoid-inertial oscillations' or, more briefly, 'inertial oscillations', which these properties make possible provides

a suitable starting point for our discussion of various phenomena encountered in the study of rotating fluids.

Relative to a state of solid-body rotation with angular velocity Ω, a weak disturbance $\mathbf{u}'(\mathbf{r},t)$, $P'(\mathbf{r},t)$, $\theta'(\mathbf{r},t)$ ($\mathbf{r}$ being the position vector) of an incompressible, uniformly and steadily-rotating, inviscid fluid which is stably stratified (i.e. $\theta = \theta_0(Z)$ in the basic state and $d\theta_0/dZ > 0$, see Eqs. (2.1), (2.2) and (2.4)) satisfies the following linear equations

$$\nabla.\mathbf{u}' = 0 \quad . \quad . \quad . \quad (3.1)$$

$$\partial\mathbf{u}'/\partial t + 2\boldsymbol{\Omega}\times\mathbf{u}' = -\nabla P' + g\theta' \quad . \quad . \quad (3.2)$$

$$\partial\theta'/\partial t + W' \, d\theta_0/dZ = 0. \quad . \quad . \quad . \quad (3.3)$$

We can satisfy Eq. (3.1) by taking $\mathbf{u}' = \nabla\times\mathbf{A}$. The vorticity equation obtained by taking the curl of Eq. (3.2) (see Eq. (2.6)), namely

$$\partial\boldsymbol{\xi}'/\partial t = (2\boldsymbol{\Omega}.\nabla)\mathbf{u}' - \mathbf{g}\times\nabla\theta' \quad . \quad . \quad . \quad (3.4)$$

(where $\boldsymbol{\xi}' = \operatorname{curl}\mathbf{u}'$) then takes the form

$$\partial^2(\nabla^2\mathbf{A})/\partial t^2 + (2\boldsymbol{\Omega}.\nabla)\partial(\nabla\times\mathbf{A})/\partial t + (d\theta_0/dZ)\,\mathbf{g}\times\nabla(\nabla\times\mathbf{A})_z = 0 \quad . \quad (3.5)$$

when $d\theta_0/dZ$ is constant.

There have been many studies of the highly anisotropic oscillations satisfying the wave-equation (3.5). It is instructive to consider disturbances on a scale much less than the dimensions of the container (but large enough to ensure that viscous dissipation is negligible). Such disturbances propagate as highly-dispersive elliptically-polarized shear waves – the 'inertial-gravity waves' – with Fourier components $\exp i(\omega t - \boldsymbol{\kappa}.\mathbf{r})$ where the angular frequency ω is related to the wavenumber vector $\boldsymbol{\kappa}$ through the dispersion relationship

$$\omega^2 = [(2\boldsymbol{\Omega}.\boldsymbol{\kappa})^2 + (\mathbf{N}\times\boldsymbol{\kappa})^2]/\boldsymbol{\kappa}.\boldsymbol{\kappa}; \quad . \quad . \quad . \quad (3.6)$$

here $\mathbf{N} \equiv gN/|\mathbf{g}|$, N being the Brunt-Väisälä frequency $(g\,d\theta_0/dZ)^{\frac{1}{2}}$ (see Eckart 1960). Disturbances on larger scales, comparable with the dimensions of the boundaries of the system, such as the familiar Rossby-Haurwitz waves (see e.g. Greenspan 1968; Pedlosky 1971; Platzman 1968; Thompson 1961) behave in a more complicated way but, in common with plane waves, when $N = 0$ the angular frequency ω never exceeds 2Ω in magnitude. This maximum value is attained in inertial waves, for which by Eq. (3.6)

$$\omega^2 = (2\boldsymbol{\Omega}.\boldsymbol{\kappa})^2/\boldsymbol{\kappa}.\boldsymbol{\kappa}, \quad . \quad . \quad . \quad (3.7)$$

when the wavefronts and displacements of particles, which now move in circular orbits, are everywhere perpendicular to $\boldsymbol{\Omega}$. In accordance with Proudman's theorem (see Eq. (2.19) we have the other extreme $\omega = 0$, corresponding to steady flow, when the wavefronts are parallel to $\boldsymbol{\Omega}$, i.e. $2\boldsymbol{\Omega}.\boldsymbol{\kappa} = 0$.

Several laboratory studies of inertial oscillations are described in the literature (see Greenspan 1968). Aldridge and Toomre (1969) have reported a particularly detailed investigation based on experiments with a rigid fluid-filled spherical cavity whose rotation speed about a fixed axis was forcibly varied in a slight but sinusoidal manner about a non-zero value (see Fig. 2). Their objective was to excite inertial eigen-oscillations within the relatively low viscosity fluid through the mild pumping of the thin viscous boundary layer (see section 4 (ii) below) near the wall – the energy input to the system being represented by the term $\nu\nabla.(\mathbf{u}\times\boldsymbol{\xi})$ in Eq. (2.5) – and to measure and compare with theory some of the properties of such modes. Several distinct resonances were detected via pressure measurements made along the axis for various ratios of the excitation to the mean rotating frequency. For the three most pronounced of these modes, the observed frequency ratios Ω/ω were found to

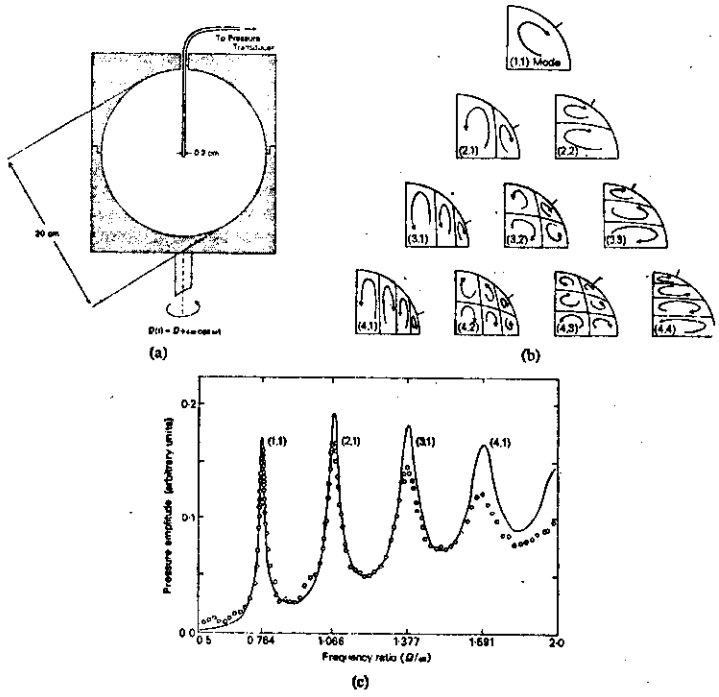

Figure 2. Axisymmetric inertial oscillations of a rotating liquid sphere (Aldridge and Toomre 1969): (a) Fluid container and pressure probe. The container (shaded), which was made of two perspex hemispheres fitted together at the equator, rotated about a vertical axis with angular speed $\Omega + \varepsilon\omega\cos\omega t$. (b) Streamlines of meridional flow for some equatorially-symmetric modes of various values of (n, m) where n is the number of modes in a 'family' and m measures the ratio of transverse to axial scale. (c) Determinations of the amplitude of the pressure oscillation at the centre of the sphere for $\varepsilon = 8{\cdot}0°$ over a range of values of Ω/ω, showing four of the seven resonance peaks detected in the experiments. The full line is based on theory, which gives the appropriate (n, m) values for each resonance.

agree with theory to better than 1%. These experiments and Aldridge's further work (Aldridge 1972) on spherical shells have proved instructive to mathematicians concerned with ill-posed problems in the theory of differential equations. As Stewartson has emphasized, in the determination of eigen-frequencies from Eq. (3.5) it is necessary to solve a hyperbolic differential equation, which has real characteristics, under boundary-conditions of the Dirichlet-Neumann type, and the absence of a general theory of such equations provides little comfort for theoreticians concerned with wave motions in atmospheres, oceans, and the earth's liquid core, where the main geomagnetic field originates. (For references see Acheson and Hide 1973; Brown and Stewartson 1976; Hide and Stewartson 1972.)

Geophysical systems such as the atmosphere and oceans are subject to the combined constraints of rotation and stable density stratification. Elementary wave motions in such

systems are the inertia-gravity waves governed by the dispersion relationship given by Eq. (3.6) when all components of κ are real. That equation also admits certain physically-acceptable oscillatory solutions with one component of κ imaginary. For example, when Ω and g are parallel (so that $z = Z$), $\kappa = (k, i\hat{l}, m)$ and $\omega^2 = N^2k^2/(k^2+m^2)$ we find

$$\hat{l} = \pm 2\Omega k/\omega = \pm 2\Omega(k^2+m^2)^{\frac{1}{2}}/N. \quad . \quad . \quad . \quad (3.8)$$

This is the solution for edge-waves confined by the interaction of buoyancy and Coriolis forces to the vicinity of a vertical wall, the presence of which is essential. Coriolis forces are everywhere balanced by pressure forces and influence the structure of the wave perpendicular to the wall and its direction of propagation along the wall, without affecting the wave frequency or the shape of the trajectories of individual fluid elements, which move in straight lines parallel to the wall. These so-called 'Kelvin waves' were first discussed in connection with the interpretation of tidal records at ports on either side of the English Channel (see Krauss 1973). They are readily produced in the laboratory and they have been invoked in the interpretation of wind observations in the tropical stratosphere, where, so far as wave motions are concerned, the change in sign at the equator of the vertical component of the earth's angular velocity vector introduces constraints roughly analogous to those imposed by the presence of a rigid impermeable wall. (See note added in proof on page 28.)

We have seen that setting $\omega = 0$ in Eq. (3.7), which applies when the fluid is homogeneous, yields the Proudman theorem and it is of interest to establish the corresponding result for a stably-stratified fluid. By Eq. (3.6), when $\omega = 0$ we have

$$(2\Omega.\kappa)^2 = -(\mathbf{N}\times\kappa)^2 \quad . \quad . \quad . \quad (3.9)$$

which cannot be satisfied unless κ has both real and imaginary components. If, for example, the disturbance has a real horizontal wavelength λ_H then its amplitude falls off exponentially in the axial direction with an e-folding scale

$$\sim \Omega\lambda_H/\pi N, \quad . \quad . \quad . \quad . \quad (3.10)$$

whereas in the case when the disturbance has an axial wavelength λ_A, the disturbance is confined to a region of horizontal dimensions

$$\sim N\lambda_A/4\Omega\pi, \quad . \quad . \quad . \quad (3.11)$$

the so-called 'Rossby radius of deformation', which gives the scale of some of the main energetic eddies in the atmosphere and oceans. By Eq. (3.9), when geostrophic balance obtains the axial and horizontal scales are roughly in the ratio $2\Omega/N$ (Prandtl's 'ratio of scales', see Prandtl 1952, also Lineykin 1974), which goes to infinity when $N \to 0$, in accordance with Proudman's theorem.

4. Steady source-sink flows

(i) *Strictly two-dimensional systems.* The inertial oscillations considered in section 3 depend for their existence on the deflecting action of Coriolis forces on moving particles, so it is appropriate to inquire whether there could be circumstances in which rotation merely changes the pressure field, leaving unaffected the trajectories of individual fluid elements relative to the rotating frame. Mechanically-driven flows which, by virtue of the boundary conditions and the supposition that the fluid is homogeneous, are two-dimensional in planes perpendicular to the axis of rotation, have this property when, in addition, a certain quantity j is equal to zero. Here j is defined as the number of irreducible sets of closed curves that can be drawn in the region of (x, y) space of connectivity c occupied by the fluid across which the net flow of fluid does not vanish. In other words, Taylor's theorem (see section 2(iv), especially Eqs. (2.11) and (2.12)) holds when the flow is driven by relative

movement of two-dimensional boundaries and/or by sources and sinks of the 'dipole' type, but not when sources and sinks of the 'monopole' type are present.

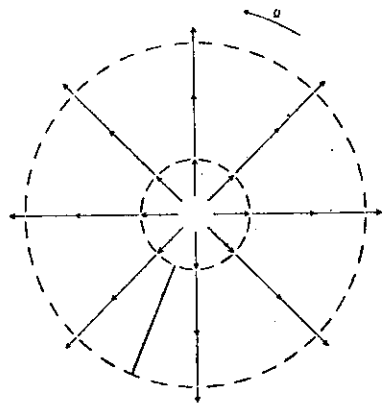

Figure 3. Streamlines of two-dimensional source-sink flow in a rotating annular system of inner radius a and outer radius b when, owing to the presence of a radial barrier (at $\phi \neq 250°$), $j = 0$, $c = 1$ (see text).

Examples of source-sink systems of both $j \neq 0$ and $j = 0$ types are illustrated by Figs. 1, 2 and 3 of Hide (1968), in each of which fluid enters and leaves the system via permeable but rigid portions of the cylindrical side-walls at a total rate $Q\,\mathrm{m^3s^{-1}}$. Fig. 3 of the present paper illustrates a system of the $j = 0$ type in the simplest case of all, where the source-sink distribution is independent of the azimuthal angle ϕ. The velocity field is determined virtually everywhere by considerations of continuity (see Eq. (2.1)) when viscous effects are confined to thin boundary layers on the rigid impermeable radial barrier connecting the two cylindrical surfaces. Thus

$$\mathbf{u} = (u_r, u_\phi, u_z) = (q/2\pi r, 0, 0) \quad . \quad . \quad . \quad (4.1)$$

where r is the radial coordinate and q times the length of the system in the z-direction is equal to Q, and the corresponding azimuthal component of the pressure gradient is given by

$$r^{-1}\,\partial P/\partial\phi = r^{-1}(\Omega q/\pi) \quad . \quad . \quad . \quad (4.2)$$

(see Eq. (2.12)). The last equation shows immediately why the radial barrier is an essential feature of the system when $\Omega \neq 0$, for without the barrier, across which a pressure difference $2\Omega\bar{\rho}q$ develops, it would be impossible to support the azimuthal pressure gradient.

When $j \neq 0$ (as in the cases illustrated by Fig. 2 of Hide (1968)) rotation interacts with the basic source-sink flow to produce j gyres, a 'cyclonic' one around each distinct sink and an 'anticyclonic' one around each distinct source. The simplest case of all (see Fig. 4) corresponds to the system illustrated by Fig. 3 with the radial barrier removed, thus increasing the connectivity c from 1 to 2 and j (which in general satisfies $j \leqslant c-1$) from 0 to 1. With no radial barrier present there can be no azimuthal pressure gradient to prevent the sideways deflection of the flow by Coriolis forces. The resulting azimuthal motion can be calculated exactly; thus $\mathbf{u} = (u_r, u_\phi, u_z)$ where $u_r = q/2\pi r$, $u_z = 0$ and

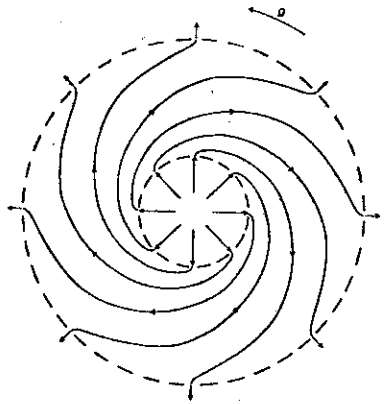

Figure 4. Streamlines of two-dimensional source-sink flow in a rotating annular system of inner radius a and outer radius b when, owing to the absence of a radial barrier (cf. Fig. 3), $j = 1$, $c = 2$ (see text).

$$u_\phi = \Omega\left\{-r+\frac{1}{b^{S+2}-a^{S+2}}\left(\frac{b^2a^2(b^S-a^S)}{r}+(b^2-a^2)r^{S+1}\right)\right\} \quad . \quad (4.3)$$

if a and b are the radii of the inner or outer cylindrical surfaces respectively and $S \equiv q/2\pi\nu$ (ν being the coefficient of viscosity and q reckoned positive or negative according as the inner cylinder is the source or sink of fluid (cf. Eq. (4.1)). Fig. 5 illustrates the dependence of the radial profile of u_ϕ on the Reynolds number $|S|$, for several values of S ranging from $-\infty$ to ∞. When $|S|$ is very small, viscosity ensures that the relative azimuthal motion u_ϕ is very slow, but when $|S| \gg 1$, viscous effects are confined to a boundary layer on the sink of thickness

$$b/S \text{ or } a/|S| \text{ according as } q \gtrless 0. \quad . \quad . \quad (4.4)$$

The azimuthal flow elsewhere is such that individual fluid elements conserve their angular momentum, so that $\zeta \equiv r^{-1}\partial(ru_\phi)/\partial r$, the axial and only non-zero component of relative vorticity $\boldsymbol{\xi}$, is equal to -2Ω; this can be seen from the general expression

$$\boldsymbol{\xi} = (0,0,\zeta) = \left(0,0,2\Omega\left\{(1+\tfrac{1}{2}S)\left[\frac{(b^2-a^2)r^S}{b^{S+2}-a^{S+2}}\right]-1\right\}\right). \quad . \quad (4.5)$$

The corresponding absolute vorticity in the main body of the fluid is zero, implying – since the area integral of the absolute vorticity can be shown to equal $2\pi(b^2-a^2)\Omega$ for all S – that when $|S| \gg 1$ the absolute vorticity is concentrated in the thin layer on the boundary where the fluid leaves the system. (This is a clear case of motions expelling absolute vorticity from the main body of the fluid and concentrating it at the rim, but by a process which can be fully specified, in contrast to some of the examples invoked during the controversy – still apparently unsettled (but see McEwan 1976) – started in the 1960s by certain speculations concerning the early stages in the development of hurricanes.)

(ii) *End-effects due to Ekman boundary layers.* Strictly two-dimensional flows are impossible to realize in practice, owing to the presence of end-walls in $z = z_l$ and $z = z_u$ (where $z_u > z_l$). The 'end-effects' produced by such walls range from minor local modifications when the basic two-dimensional flow has no relative vorticity and the end-walls are

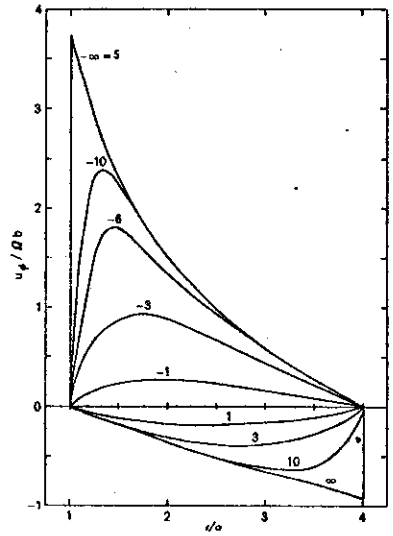

Figure 5. The variation of azimuthal velocity u_ϕ with radius r for the system illustrated by Fig. 4 when $b = 4a$, calculated for several values of $S \equiv q/2\pi\nu$, $|S|$ being a Reynolds number based on the source strength. When $|S| \gg 1$ individual fluid particles tend to conserve their angular momentum as they traverse the main body of the system, the corresponding relative vorticity ζ being close to -2Ω. A boundary layer of thickness b/S when $S > 0$ (and $a/|S|$ when $S < 0$) and in which $\zeta \sim |S|\Omega$ forms on the surface of the sink, but there is no corresponding boundary layer on the surface of the source.

everywhere perpendicular to $\boldsymbol{\Omega}$ (i.e. when $\nabla_1 z_l(r,\phi) = \nabla_1 z_u(r,\phi) = 0$), to major changes in the flow pattern throughout the whole system when the basic two-dimensional flow possesses vorticity or the end walls are not everywhere perpendicular to $\boldsymbol{\Omega}$.

Consider first the case when the end-walls are perpendicular to $\boldsymbol{\Omega}$, so that $\nabla_1 z_l = \nabla_1 z_u = 0$ and the separation distance

$$D \equiv z_u(r,\phi) - z_l(r,\phi) \quad . \quad . \quad . \quad (4.6)$$

is uniform (cf. Fig. 6). Supposing that the coefficient of kinematic viscosity ν, though non-zero, is so small that the boundary layers that develop on each end-wall so as to satisfy the no-slip boundary condition there are small in thickness δ (i.e. $\delta \ll D$), we can readily show that

$$\delta = (\nu/\Omega)^{\frac{1}{2}}(1+O(\varepsilon)) \quad . \quad . \quad . \quad (4.7)$$

where ε is the Rossby number (see Eq. (2.16)), implying that when the interior flow is quasi-geostrophic (i.e. $\varepsilon \ll 1$ and $E \ll 1$, see Eq. (2.17)) the boundary-layer is highly ageostrophic with the 'Ekman' structure. The components (u_1, u_2) of $\mathbf{u}$ parallel to the wall are given by

$$u_1 = \{U_1(1-e^{-\sigma}\cos\sigma) \mp U_2 e^{-\sigma}\sin\sigma\}(1+O(\varepsilon)) \quad . \quad (4.8)$$

and

$$u_2 = \{U_2(1-e^{-\sigma}\cos\sigma) \pm U_1 e^{-\sigma}\sin\sigma\}(1+O(\varepsilon)) \quad . \quad (4.9)$$

where (U_1, U_2) are the corresponding quasi-geostrophic components at the edge of the

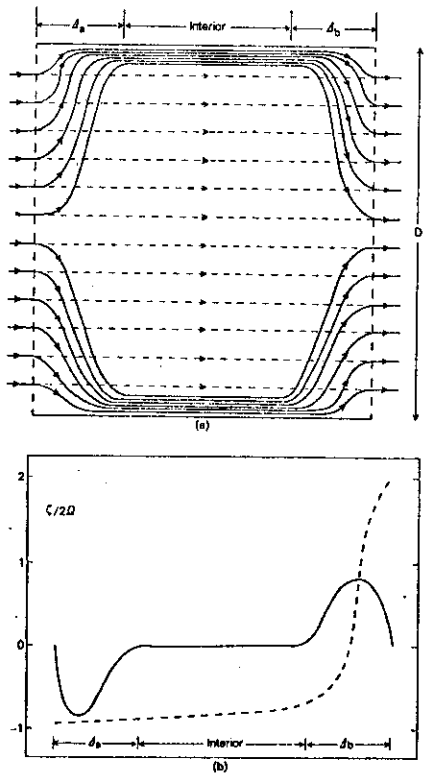

Figure 6. Illustrating the effect of end-walls separated by a uniform distance D on flows due to distribution of sources and sinks for which $j \neq 0$ (see text), as exemplified by the simple case of an annular system (see Figs. 4 and 5) with $j = 1$. (a) shows the projection of streamlines on a meridian plane and (b) shows the corresponding radial variation of relative vorticity ζ in regions remote from the Ekman boundary layers of thickness $\delta = (\nu/\Omega)^{\frac{1}{2}}$ on the end-walls. The lightly-dashed line corresponds to the case when the end-walls are absent and the full line to the case when the end-walls are present. Suction due to the Ekman boundary layers reduces the radial motion u_r and the relative vorticity ζ to zero in the main body of the fluid and gives rise to axial motion in boundary layers of thickness Δ_a and Δ_b on the side-walls.

boundary layer, where it meets the interior region, σ is a 'stretched' coordinate equal to x_3, the distance from the boundary, divided by δ, and the upper (lower) sign is taken when Ω is parallel (antiparallel) to the positive x_3-direction. There is a net cross-isobar flow in the boundary layer, and if the x_3-component of the vorticity in the interior region, $\partial U_2/\partial x_1 - \partial U_1/\partial x_2$, is non-zero, boundary layer 'suction' occurs, giving rise to a value of u_3, the component of $\mathbf{u}$ normal to the boundary, which vanishes on the rigid boundary only and has the generally non-zero value

$$U_3 = \pm\tfrac{1}{2}\delta(\partial U_2/\partial x_1 - \partial U_1/\partial x_2)(1+O(\varepsilon)) \quad . \quad . \quad (4.10)$$

at the edge of the boundary layer (see e.g. Batchelor 1967; Greenspan 1968; Prandtl 1952).

Returning to the discussion of source-sink flows, we find that U_3 vanishes in all cases of such systems having $j = 0$ (as exemplified by Fig. 3), for in such cases the basic relative vorticity $\partial U_2/\partial x_1 - \partial U_1/\partial x_2 = \pm\zeta = 0$ (where $\zeta = r^{-1}\partial(ru_\phi)/\partial r - r^{-1}\partial u_r/\partial\phi$). The end-walls boundary layers are then passive in the sense that they merely reduce the relative flow from its non-zero value in the interior region to zero on the wall, where the no-slip boundary condition must be satisfied. This behaviour contrasts sharply with cases when $j \neq 0$ (as exemplified by Fig. 4), where $\zeta \neq 0$ and boundary layer suction completely changes the interior solution and gives rise to complicated three-dimensional boundary-layers on the side-walls (see Fig. 6).

The modified flow in the latter case consists of five regions (see Fig. 6): the inviscid region, in which the flow is quasi-geostrophic when $\varepsilon \ll 1$ and $E \ll 1$, satisfying

$$\mathbf{u} = (u_r, u_\phi, u_z) = (0, \quad Q\Omega^{\frac{1}{2}}/2\pi\nu^{\frac{1}{2}}r, \quad 0)(1+O(\varepsilon)) \quad . \quad (4.11)$$

(where $\varepsilon = Q/2\pi\nu^{\frac{1}{2}}\Omega^{\frac{1}{2}}a^2 = Q/2\pi\delta\Omega a^2$ and $E = \delta^2/D^2$), and four highly ageostrophic regions (see section 2(v)) comprising two Ekman layers of thickness δ on the end-walls separated by the uniform distance D and boundary layers of thickness Δ_a and Δ_b on the side-walls in $r = a$ and $r = b$, supposing that $\Delta_a + \Delta_b \ll b - a$. The transfer of fluid now takes place via these boundary layers, but it is theoretically significant that simple Ekman theory, without recourse to consideration of the complex structure of the side-wall boundary layers, can be used to determine $\mathbf{u}$ in the inviscid interior with an error no more than $O(\varepsilon)$. Within that region all components of relative vorticity $\boldsymbol{\xi}$ now vanish (to $O(\varepsilon)$) – in contrast to the case when the end-walls are absent, see Fig. 5 – since Proudman's theorem (see Eq. (2.19)) requires that geostrophic flow of a homogeneous fluid should satisfy $\partial\mathbf{u}/\partial z = 0$, the first two components of which when combined with Eq. (4.10) give

$$\partial u_z/\partial z = -\delta\zeta/D \quad . \quad . \quad . \quad (4.12)$$

which is only compatible with the third component $\partial u_z/\partial z = 0$ when $\zeta = 0$.

The mathematical analysis of the side-wall boundary layers is highly complex, even in the case when non-linear effects are negligible and the layers are consequently of the so-called 'Stewartson-type' with overall thickness $(D\delta/2)^{\frac{1}{2}}$ (and therefore proportional to $\nu^{\frac{1}{4}}$) and sub-structure on a scale $D^{\frac{1}{4}}\delta^{\frac{3}{4}}$ (proportional to $\nu^{\frac{1}{2}}$). Unfortunately, the error in the linear theory is $\sim a\varepsilon/D^{\frac{1}{4}}\delta^{\frac{3}{4}}$ or $b\varepsilon/D^{\frac{1}{4}}\delta^{\frac{3}{4}}$, implying that non-linear effects must be taken into account in the treatment of the side-wall boundary layers even when linear (Ekman) theory suffices for the end-wall boundary layers. According to an approximate analysis (Hide 1968) of an axisymmetric system (see Fig. 6) and a supporting laboratory investigation, the thickness of the boundary layer on the source (Δ_a when $q > 0$) increases and that of the sink boundary layer (Δ_b when $q > 0$) decreases with increasing $\varepsilon E^{-\frac{1}{2}}$ (and vice versa when $q < 0$), but in such a way that the product $\Delta_a\Delta_b$ remains $\sim D\delta/2$ even when $\varepsilon E^{-\frac{1}{2}}$ is quite large, with Δ_b tending to the value $2\pi vbD/Q$ (see Eq. (4.4) and Fig. 5) and Δ_a to $Q/4\pi\nu^{\frac{1}{2}}\Omega^{\frac{1}{2}}a$ when $\varepsilon E^{-\frac{1}{2}} \gg 1$. These results have been generally confirmed and extended by further work, including a combined numerical and laboratory investigation by Bennetts and Jackson (1974).

Because the flow is axisymmetric, it is a relatively straightforward matter to extend the foregoing analysis to cases when the end-walls are no longer perpendicular to Ω provided that in shape they remain figures of revolution about the axis of symmetry, since differences from the case illustrated by Fig. 6 are then mainly only quantitative. Thus, when the bounding end-wall surfaces are concentric spheres of radii $\hat{a}$ and $\hat{b}(\hat{b} > \hat{a})$ (see Fig. 7) and relative flow is produced by a cylindrical source near one pole feeding a cylindrical sink near the other pole, the transfer of fluid, again, takes place via Ekman layers, which now have thickness

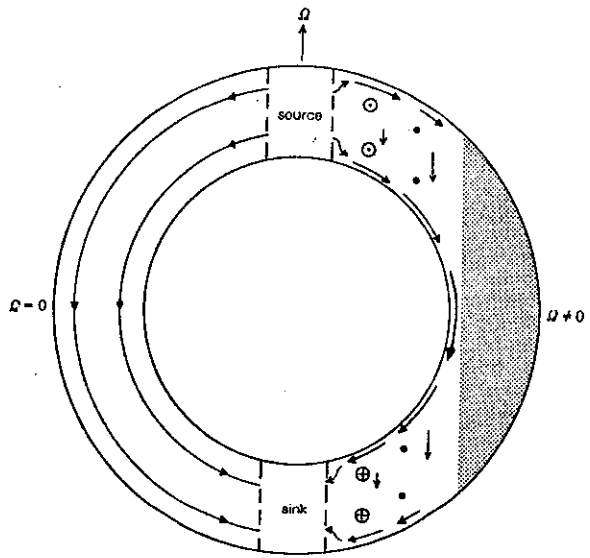

Figure 7. Axisymmetric source-sink flow in a spherical shell of fluid. The left side of the schematic diagram shows the streamlines for the case when the basic angular speed of rotation $\Omega = 0$. Fluid then moves directly from the source in the northern hemisphere to the sink in the southern hemisphere, with individual elements following trajectories for which $r^2 + z^2 =$ constant. This flow pattern should be compared with that found in the rapidly-rotating case illustrated by arrows on the right side of the diagram. The transfer of fluid now takes place via Ekman boundary layers on the inner and outer spherical boundaries. Whilst the transfer via the boundary layer on the outer sphere decreases with decreasing latitude, that via the boundary layer on the inner sphere increases with decreasing latitude (see Eq. (4.13)) and continuity requires that there should be a compensating axial component to the flow in the interior region (see Eq. (4.14)). The azimuthal flow in the interior region is in geostrophic balance and vanishes, in accordance with Proudman's theorem (Eq. (2.19)) and the Ekman suction formula (Eq. (4.11)), in the stippled region where r exceeds the radius of the inner sphere.

$$\delta = \nu/(\Omega|\cos\psi|)^{\frac{1}{2}} \quad . \quad . \quad . \quad (4.13)$$

where ψ is the 'co-latitude', so that δ increases with increasing distance from the poles. Owing to this ψ-dependence of δ, at a given distance r from the axis the boundary layer on the outer sphere is thinner than the layer on the inner sphere and therefore transports less fluid towards the equator. In contrast to the cylindrical case illustrated by Fig. 4, continuity demands an axial flow u_z in the inviscid interior where u_z is independent of the axial co-ordinate (in keeping with the third component of Eq. (2.19)) and varies with r according to the expression

$$u_z(r) = \frac{Q}{4\pi\hat{b}^2\hat{a}^2}\left\{\frac{\hat{a}^2(1-r^2/\hat{a}^2)^{\frac{1}{2}}(1-r^2/\hat{b}^2)^{-\frac{1}{2}} - \hat{b}^2(1-r^2/\hat{b}^2)^{\frac{1}{2}}(1-r^2/\hat{a}^2)^{-\frac{1}{2}}}{(1-r^2/\hat{a}^2)^{\frac{1}{2}}+(1-r^2/\hat{b}^2)^{\frac{1}{2}}}\right\} \quad (4.14)$$

when $r < \hat{c}$, the azimuthal motion being related to u_z by the Ekman suction formula given by Eqs. (4.10) and (4.13). A striking feature of the flow is the absence in this geostrophic

limit of any motion in the fluid occupying the region between the imaginary cylindrical surface $r = \hat{a}$ and the 'low-latitude' part of the outer bounding sphere which extends from $r = \hat{a}$ to the 'equator' at $r = \hat{b}$. The geostrophic azimuthal flow in the region $r \leqslant \hat{a}$ drops to zero at $r = \hat{a}$ but its rate of change with respect to r does not, implying that a weak ageostrophic detached shear layer will be present near $r = \hat{a}$. This layer and the boundary layers on the cylindrical surfaces of the source and sink as well as the boundary layer at the equator of the inner sphere, where Ekman theory breaks down (as evinced by the behaviour of the r.h.s. of Eq. (4.13) when $\psi = \pi/2$) are complex in structure and their theoretical investigation poses some very difficult mathematical problems. Again, however, the flow elsewhere can be determined by elementary theoretical considerations and unpublished experiments carried out in my laboratory demonstrate conclusively that this flow occurs in practice. (The study of source-sink flows is not, of course, directly relevant to dynamical meteorology, but it is nevertheless interesting to note that the tendency for the main constituent of the Martian atmosphere, carbon dioxide, to freeze out near the winter pole gives rise to a net poleward atmospheric flow and a concomitant increase in azimuthal wind speed; for references see e.g. Golitsyn 1973 or my Presidential Address for 1975 (Hide 1976).)

(iii) *Geostrophic contours and end-effects due to topography.* We now turn to the more complicated general case of non-axisymmetric system for which the axial distance D (see Eq. (4.6)) between the end-walls is non-uniform. We have seen in section 2 (see Eq. (2.23)) that in quasi-geostrophic flow of a homogeneous incompressible fluid, such as the interior flows in the cases discussed in (ii) above, changes in relative vorticity are brought about mainly by axial stretching, and indeed the axial vorticity in the side-wall boundary layers in the flow illustrated by Fig. 6 is strongly influenced by axial stretching due to Ekman boundary-layer suction at the end-walls. When, in addition to Ekman suction, end-wall topography contributes to axial stretching, by Eqs. (2.23), (2.19) and (4.12), the axial component of the quasi-geostrophic relative vorticity, ζ, satisfies

$$\partial\zeta/\partial t + (\mathbf{u}_1.\nabla_1)\zeta \doteq 2\Omega[(\mathbf{u}_1.\nabla_1)D - \delta\zeta]/D \quad . \quad . \quad (4.15)$$

The relative importance of the topographic contribution to vorticity changes, as represented by the term $2\Omega D^{-1}(\mathbf{u}_1.\nabla_1)D$ in Eq. (4.15), is measured by the ratio h/h_* where h is the amplitude of variations in D and

$$h_* \sim \varepsilon D + \delta. \quad . \quad . \quad . \quad (4.16)$$

Topographic end effects will not be important when $h \ll h_*$, but when $h > h_*$ — and this is always the case for strictly geostrophic motion since h_* then vanishes — such effects are so strong that within the main body of the fluid the flow is steered (to $O(\varepsilon)$) along geostrophic contours, defined as curves on which

$$D \equiv z_u - z_l = \text{constant}. \quad . \quad . \quad . \quad (4.17)$$

Another solution of the 'steering equation'

$$\mathbf{u}_1.\nabla_1 D = 0 \quad . \quad . \quad . \quad . \quad (4.18)$$

satisfied by $\mathbf{u}_1$ is $\mathbf{u}_1 = 0$, and indeed there *are* circumstances in which the effect of topography is to produce stagnation, as in the case of the equatorial region of the spherical system discussed in (ii) above (see Fig. 7). Quasi-geostrophic motion is clearly impossible in regions where, owing to the geometry of the end-walls, continuous geostrophic contours cannot be found, and within such regions the flow, if it does not vanish, either oscillates rapidly or is characterized by strong transverse shear.

The effect of axisymmetric sloping end-walls on the source-sink flow illustrated by

Fig. 3 is particularly striking (see Fig. 8) — in contrast to the case illustrated by Fig. 4 and 6, for which the basic flow is parallel to the geostrophic contours and is therefore unaffected by

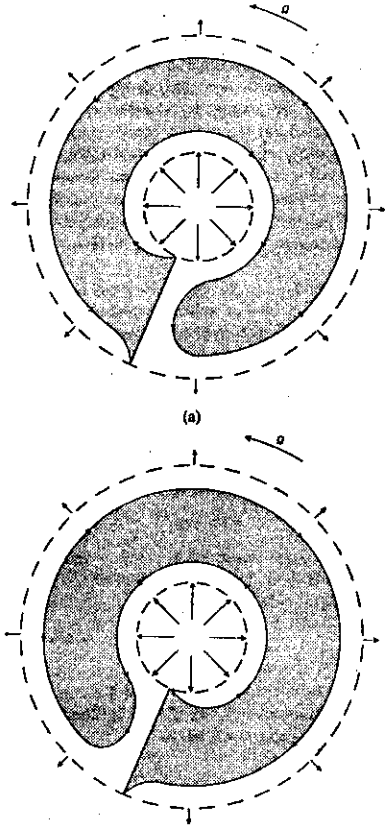

Figure 8. Schematic diagram illustrating the effect of axisymmetric sloping end-walls on flow due to a two-dimensional source-sink distribution in an annular system with a radial barrier. In the case when the distance D between the end-walls is uniform, streamlines are purely radial (see Fig. 3). Fig. 8(a) illustrates the case when $dD/dr > 0$ (see text) and Fig. 8(b) the case when $dD/dr < 0$. In the main body of the fluid there can be no flow across 'geostrophic contours' r = constant, and owing to this major constraint on the flow, motion is largely confined to highly ageostrophic boundary layers on the cylindrical surfaces of the source and sink and on one side only of the radial barrier, where the transfer of fluid from the inner cylinder to the outer cylinder takes place via a 'western boundary current' when $dD/dr > 0$ (see Fig. 8(a)) or an 'eastern boundary current' when $dD/dr < 0$ (see Fig. 8(b)). The motion simply reverses direction, with no significant change in flow pattern, when the source and sink are interchanged, so that fluid enters the system via the outer cylinder instead of the inner cylinder and vice versa.

topographic stretching. Figure 8(a) illustrates the case when D increases with increasing distance from the axis (i.e. $dD/dr > 0$) and $D(b) - D(a) \gg h_*$ (see Eqs. (4.16) and (4.18)), and Fig. 8(b) the case when $dD/dr < 0$ and $D(a) - D(b) \gg h_*$. In the main body of the fluid, there can be no flow across geostrophic contours, which are circles concentric with the axis of rotation, and, owing to this major constraint on the flow, motion is largely confined to highly ageostrophic boundary layers on the cylindrical surfaces on the source and sink and on one side or the other side of the radial barrier, where the transfer of fluid from the inner cylinder to the outer cylinder (when $q > 0$, the case illustrated) takes place in a 'western boundary current' when $dD/dr > 0$ (see Fig. 8(a)) or an 'eastern boundary current' when $dD/dr < 0$ (see Fig. 8(b)). The motion simply reverses direction, with no significant change in the general flow pattern, when $q < 0$, corresponding to the case when fluid enters the system via the outer cylinder rather than the inner cylinder. Within the 'western' or 'eastern' boundary current, the 'planetary vorticity' term $2\Omega D^{-1}(\mathbf{u}_1.\nabla_1)D$ is balanced by the sum of the non-linear advective term $(\mathbf{u}_1.\nabla_1)\zeta$ and the viscous term $\nu\nabla_1^2\zeta$ in the vorticity equation (see Eqs. (2.6), (2.11) and (4.15)).

It is possible to show that in its main dynamical effects the sloping end-walls with D increasing outwards is formally equivalent in the case of a homogeneous fluid to the latitudinal variation of the Coriolis parameter f (the vertical component of 2Ω, see Eq. (2.27)) when dealing with flow in a thin spherical shell (for references see Greenspan 1968). This is often called the 'beta-effect' in dynamical meteorology and oceanography, owing to the use of the so-called 'beta-plane' where local Cartesian coordinates are used (with the X-axis towards the east and the Y-axis towards the north) and f is taken as a linear function of Y:

$$f = f_0 + \beta Y \quad . \quad . \quad . \quad . \quad . \quad (4.19)$$

The best-known example of a western boundary current in nature is the Gulf Stream in the Atlantic Ocean (Stommel 1965), the earliest theoretical investigations of which were greatly aided by various laboratory studies of source-sink flows in systems akin to those illustrated by Figs. 8(a) and (b) (for review see Veronis 1973). Inserting a rigid full meridional barrier connecting the source to the sink in the spherical system illustrated by Fig. 7 gives rise to a cross-equatorial western boundary current reminiscent of the East-African low-level cross-equatorial jet-stream in the atmosphere and the Somali Current in the Indian Ocean.

(iv) *Other experiments with mechanically-driven flows.* Time and space do not permit the detailed treatment of further examples of experiments on basic processes in mechanically-driven systems, such as 'spin-up', which has received a great deal of attention (see Benton and Clark 1974; Buzyna and Veronis 1971; Greenspan 1968). Central to the understanding of these processes, as attested by the cases we have chosen to discuss in detail, is the Proudman theorem expressing, effectively, the tendency for slow disturbances to propagate preferentially in directions parallel to the rotation axis. The system illustrated by Fig. 6 is a convenient one for studying the disturbance produced by a localized bump on one of the end-walls or by a solid object placed in the interior region. The wake due to the presence of such an obstacle to the flow takes the form of a 'Taylor column' trailing at an angle $\sim\varepsilon$ radians to the z-axis when $\varepsilon \ll 1$ (see Hide *et al.* 1968). In the 'viscous' limit when $\varepsilon \ll E^{\frac{1}{3}}$ ($\ll 1$) the column is parallel to the z-axis, the flow within it is virtually stagnant, and the 'walls' of the column are highly ageostrophic detached shear layers of thickness $\sim (D\delta)^{\frac{1}{2}}$ (see Greenspan 1968). Otherwise, i.e. when $E^{\frac{1}{3}} \ll \varepsilon$ ($\ll 1$) the Taylor column is of the so-called 'inertial type' and much more complicated in structure than in the viscous limit.

Recent studies of Taylor columns have included work on effects due to density stratification. On the experimental side, the combined effects of rotation and stratification are probably best studied by determining the flow produced by moving solid objects slowly through a fluid which otherwise rotates uniformly, as in Taylor's pioneering study of

homogeneous systems (see Taylor 1923, 1974). Various lines of theoretical and experimental evidence indicate that stratification restricts the penetration distance parallel to the rotation axis to a value given by Eq. (3.10) when the advective contribution to ageostrophic effects is more important than viscosity (for references see Mason 1976). The study of flow over and around topography in rotating non-homogeneous fluids is currently an active area of research in geophysical fluid dynamics and should in due course provide dynamical oceanographers and meteorologists with a better foundation for interpreting observations and with improved methods of representing effects due to topography in numerical models.

Experimental and theoretical investigations of channel flows have also featured in recent work. These studies, which include important generalizations of hydraulic theory to the case of rotating fluids, bear on certain problems in dynamical oceanography (see e.g. Stern 1975).

In our discussion thus far we have encountered several examples of highly ageostrophic shear layers on end-walls and side-walls and detached shear layers in the main body of the fluid. As a rule, instabilities develop on these shear layers when an appropriate Reynolds number based on the thickness of the layer exceeds a critical value $\gtrsim 10$, and experimental investigations have played a leading role in the study of these instabilities. Important work on Ekman layer instability has been carried out using systems essentially of the type illustrated by Fig. 6, and the stability of detached shear layers and of western boundary currents has been usefully investigated in systems driven by differential rotation between part or the whole of the upper end-wall and the other bounding surfaces (for references see Greenspan 1968).

5. Thermally-driven flows due to an impressed horizontal temperature gradient

Having considered a variety of mechanically-driven flows we conclude our discussion of experiments with rotating fluids with a brief account of systems driven by buoyancy forces due to impressed differential heating and cooling. For theoretical purposes it is often convenient to specify the impressed heating and cooling in terms of the hypothetical temperature field $T_i(\mathbf{r}, t)$ corresponding to the actual temperature field that would obtain if the fluid in the system were replaced by a solid of the same thermal properties. Corresponding to $T_i(\mathbf{r}, t)$ is a hypothetical density field specified by $\theta_i(\mathbf{r}, t)$, where θ is related to T through the thermal coefficient of cubical expansion $-d\theta/dT$.

By Jeffreys' theorem (see Eq. (2.6)), hydrostatic equilibrium obtains in the special case when the horizontal gradient of θ_i vanishes everywhere (and there is no mechanical forcing), but the equilibrium is unstable when the vertical gradient is anywhere top heavy (i.e. $d\theta_i/dZ < 0$) and sufficiently large in magnitude to overcome dissipative effects due to viscosity, thermal conduction, etc. The investigation of the ensuing overturning motions, as exemplified by the well-known phenomenon of Bénard convection, has been the subject of a considerable amount of experimental and theoretical work (for references see Busse and Carrigan 1974; Chandrasekhar 1961; Gilman 1975; Spiegel 1972; Turner 1973), and this has included cases when general rotation is so rapid that Coriolis forces play a dominant role.

In the more general case when the impressed temperature gradient is not entirely vertical, fluid motions occur for all values of $\partial\theta_i/\partial Z$ for (by Jeffreys' theorem) $\mathbf{g} \times \nabla\theta_i \neq 0$ and hydrostatic equilibrium is consequently impossible. It is with such systems in cases when the ensuing motions are strongly influenced by Coriolis forces due to rapid rotation that this final section is largely concerned. These motions not only carry heat horizontally, thereby reducing the impressed horizontal temperature gradient, but they also carry heat

upwards, thereby *increasing* the upward component of the temperature gradient and the downward component of the density gradient.

Thermally-driven flows in rotating fluids subject to a horizontal temperature gradient have been studied extensively during the past twenty-five years (for references see Hide and Mason 1975). Many of the experimental findings are evidently quite general and therefore of wide theoretical interest, and on the meteorological side these findings were influential in the development of successful ideas concerning the large-scale motions in the atmosphere (see Lorenz 1967; Quinet 1974), at a time when such problems were well beyond the range of computers. Indeed, even modern computers are at a disadvantage in the investigation of the more complicated flow phenomena encountered — at first sight somewhat paradoxically — when the apparatus is rotated comparatively rapidly (see Eqs. (5.2) and (5.3) and Fig. 10).

The simplest system in which controlled and reproducible experiments have been carried out is the annular apparatus introduced by Hide in 1950 (see Fig. 9) for which, in the case when there are no internal heat sources ($\tilde{Q} = 0$ in the notation of Eq. (2.3)) but the bounding cylindrical side-walls in $r = a$ and $r = b$ are maintained at different temperatures T_a and T_b respectively, the impressed temperature field satisfies

$$T_i = [T_b \ln(r/a) - T_a \ln(r/b)]/\ln(b/a). \qquad (5.1)$$

Accurate determinations of the principal spatial and temporal characteristics of the fields of temperature and flow velocity over a wide range of precisely specified and carefully-controlled experimental conditions led to the discovery of several fundamentally different free types of flow (see Table 1), only one of which is symmetrical about the axis of rotation (see Fig. 10). The general character of the flow evidently depends largely on the values of certain external dimensionless parameters:

$$\Theta \equiv gd\Delta\rho/\bar{\rho}\Omega^2(b-a)^2 \qquad (5.2)$$

and

$$\mathscr{T} \equiv 4\Omega^2 l_4/\nu^2, \qquad (5.3)$$

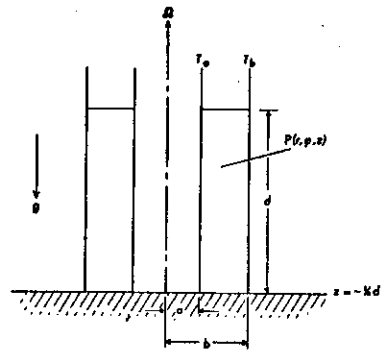

Figure 9. Schematic diagram of a rotating fluid annulus subject to a horizontal temperature gradient, drawn for the case when the upper and lower bounding surfaces are horizontal. P is a general point with polar coordinates (r, ϕ, z) in a frame of reference rotating with the apparatus. $\Omega = (0, 0, \Omega)$ is the angular velocity of basic rotation; $\mathbf{g} = (0, 0, -g)$ is the acceleration of gravity (which in magnitude is typically very much larger than $\Omega^2 r$); the region occupied by the fluid is $a < r < b$ and $-\frac{1}{2}d < z < \frac{1}{2}d$; T_a and T_b denote the respective temperatures at which the inner and outer cylindrical boundaries are held by means of temperature baths.

TABLE 1. BROAD CLASSIFICATION OF MODES OF FREE CONVECTION IN A ROTATING FLUID IN AN AXISYMMETRIC CONTAINER SUBJECT TO A HORIZONTAL TEMPERATURE GRADIENT

(1) AXISYMMETRIC

(2) NON-AXISYMMETRIC
- (a) regular baroclinic waves
  - (i) steady waves
  - (ii) 'vacillation' (wave shape, wave amplitude, wave number, wave dispersion)
- (b) irregular baroclinic waves (geostrophic turbulence)

where g is the acceleration of gravity and typically $\gg \Omega^2 b$, d the depth of the fluid, $\Delta\rho$ the density contrast associated with the impressed density difference, i.e. $\Delta\rho \equiv |\rho(T_a) - \rho(T_b)|$, $\bar{\rho}$ is the mean density, Ω the angular velocity of basic rotation and ν the kinematic viscosity

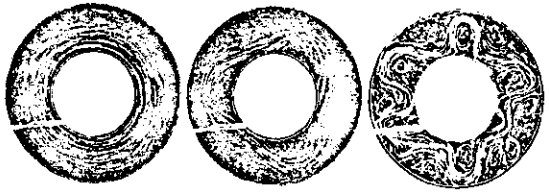

Figure 10. Streak photographs giving one example of each of the main modes of thermal convection in a rotating fluid annulus subject to a horizontal temperature gradient (see Figs. 9 and 11), namely (a) axisymmetric flow, (b) regular baroclinic waves and (c) irregular baroclinic waves, corresponding to different rates of (anticlockwise) basic rotation rate $\Omega = 0{\cdot}341$, $1{\cdot}19$ and $5{\cdot}02\,\mathrm{rad\,s^{-1}}$ respectively. (Experimental details: $a = 3{\cdot}8\,\mathrm{cm}$; $b = 8{\cdot}4\,\mathrm{cm}$; $d = 15{\cdot}4\,\mathrm{cm}$; $T_a = 16{\cdot}3°\mathrm{C}$; $T_b = 25{\cdot}8°\mathrm{C}$; working fluid – water; duration of time exposure for streak photographs was 1 s for Fig. 10(a) and 3 s for Figs. 10(b) and (c).) Note that the thick white streak in the lower left quadrant of each picture has no significance; it is the outline of a wire well above the surface of the fluid. (Taken from a review by Hide 1969.)

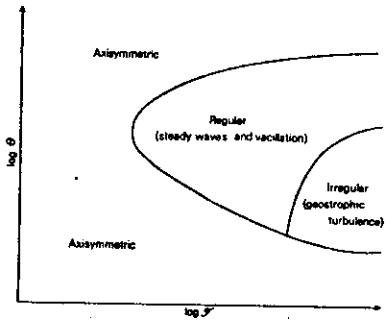

Figure 11. Schematic regime diagram illustrating the dependence of the mode of thermal convection in a rotating fluid annulus subject to a horizontal temperature gradient on the two principal dimensionless parameters required to specify the system, namely Θ and $\mathscr{T}$ (see Eqs. (5.2) and (5.3), Table 1 and Fig. 10).

of the fluid. The quantity l_4 has the dimensions of length to the fourth power and over a fairly wide range of conditions is equal to $(b-a)^5/d$. When $\mathscr{T}$ is less than a certain critical value of about 2×10^5 (see Fig. 11), viscosity ensures that the motion is essentially symmetrical about the axis of rotation for all values of Θ (cf. Fig. 10(a)), but when $\mathscr{T}$ exceeds this critical value there exists a certain range of Θ within which the corresponding motions are highly non-axisymmetric and either regular (cf. Fig. 10(b)) or irregular (cf. Fig. 10(c)), depending on the values of Θ and $\mathscr{T}$. The regular flows (as exemplified by Fig. 10(b)) usually exhibit periodic time variations which take the form of 'vacillations' (see Hide 1953, 1958) in wave-amplitude, wave-shape, or wavenumber, or of wave dispersion (see Table 1), but under certain conditions the amplitude of these periodic changes is so small that, apart from a steady drift of the wave pattern relative to the apparatus, the flow is virtually steady. In sharp contrast to this behaviour, the irregular flows, as exemplified by Fig. 10(c), exhibit complicated aperiodic fluctuations.

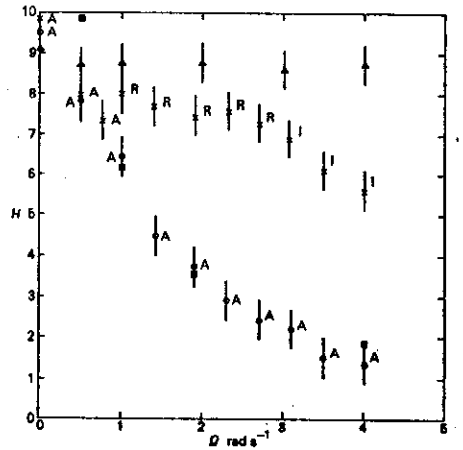

Figure 12. Illustrating the dependence of the heat transfer coefficient H (Nusselt number) on the basic rotation rate Ω for thermal convection in a typical rotating fluid annulus subject to a horizontal temperature gradient (see Figs. 9, 10 and 11 and Table 1). $H = 1$ corresponds to no convective heat transfer, just conduction (and radiation). The letter 'A' denotes axisymmetric flow, 'R' regular baroclinic waves and 'I' irregular baroclinic waves ('geostrophic turbulence'). Crosses on the error bars correspond to a system with plane horizontal end-walls, circles to sloping end-walls introduced so as to suppress non-axisymmetric flow (see Hide and Mason 1975) and triangles to a case when a rigid impermeable full radial barrier connecting the inner and outer cylinder was inserted so as to reduce the effect of rotation on advective heat transfer. The squares are values based on a simple theoretical model of heat transfer due to axisymmetric flow (Hide 1967) and are evidently in good agreement with the experimental measurements.

Here is not the place to present a detailed account of extensive experimental and theoretical work on various aspects of these flow phenomena (for reviews see e.g. Fultz *et al.* 1959; Hide 1969; Hide and Mason 1975), but it is of some interest to discuss certain findings that bear on the basic theoretical ideas presented in section 2. Of particular interest is the effect of rotation on heat transfer (see Fig. 12). In a system characterized by axial symmetry about the rotation axis, motions are confined to meridian planes when $\Omega = 0$, with lighter (warm) fluid rising and passing from the warm side to the cold side, and heavier (cool) fluid

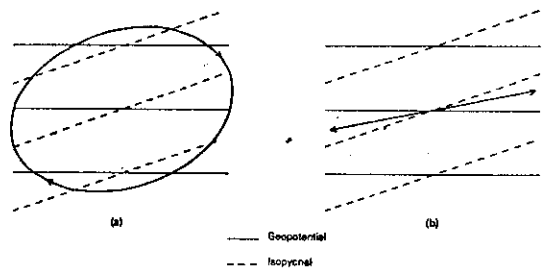

Figure 13. Illustrating 'sloping convection' (see text). In case (a), Ω is zero or sufficiently small for direct axisymmetric meridional overturning to occur as a result of the impressed horizontal density gradient. At higher rates of rotation, case (b), Coriolis forces inhibit direct meridional overturning, and the motion now consists of non-axisymmetric baroclinic waves, or 'sloping convection', with motions and variations in the velocity, pressure and density field having ϕ components, perpendicular to the plane of the diagram. Typical individual fluid elements move in trajectories that are only slightly inclined to the horizontal at an angle which is essentially non-zero but less than the slope of the isopycnic surfaces, so as to ensure that on average denser fluid sinks and lighter fluid rises.

sinking and passing from the cool side to the warm side. Under the action of gravitational torques proportional to $\mathbf{g} \times \nabla\theta$ (see Eq. (2.6)), fluid elements undergo an overturning motion (see Fig. 13(a)), the associated vorticity vector being azimuthal in direction. When, on the other hand, $\Omega \neq 0$, gyroscopic torques proportional to $(2\Omega.\nabla)\mathbf{u}$ arise and these inhibit meridional overturning. Indeed, the inhibition is complete when Coriolis forces greatly exceed the other inertial forces and viscous forces, as they would in the main body of a rapidly rotating fluid (though not in viscous boundary layers or detached shear layers); the essential torque balance is then given by the thermal wind equation (2.18), from which it follows that $\mathbf{u}$ is then mainly horizontal in direction everywhere if it is horizontal on the boundaries. Axisymmetric motions satisfying the geostrophic equations are highly inefficient not only at converting kinetic potential energy into kinetic energy, a process that requires overturning motions (see Eq. (2.5)), but also at advecting heat in directions perpendicular to Ω, since u_ϕ vanishes when $\mathbf{u}$ satisfies Eq. (2.15) with $\partial P/\partial\phi = 0$. Horizontal advective heat transfer by axisymmetric motions will take place largely in the end-wall Ekman layers (see Eqs. (4.7)–(4.9)) and such transfer decreases rapidly with Ω, roughly as $\Omega^{-\frac{1}{2}}$ (Hide 1967). One therefore expects, and the experiments confirm, that if the flow were to remain axisymmetric as Ω increases, the advective contribution $H-1$ (when expressed in suitable dimensionless units) to the heat transfer should become vanishingly small (see Fig. 12). (Here H is the Nusselt number, defined as the total heat transfer divided by the heat transfer by conduction (and/or radiation) alone (see e.g. Hide 1958; Krieth 1968).)

In practice, however, the flow does not remain axisymmetric, unless very special steps are taken (see Fig. 12), and the dependence of H on Ω is rather more complicated than a steady monotonic decrease. When, as a result of increasing Ω, H has dropped by no more than 20% or 30% (depending on the exact values of other parameters) below $H(\Omega = 0)$, regular non-axisymmetric wave-motions set in (see Fig. 10(b) and 11) and within the regular waves regime H remains fairly independent of Ω (see Fig. 12). It is only when Ω attains a sufficiently high value for irregular non-axisymmetric flow ('geostrophic turbulence') to occur (see Figs. 10(c) and 11) that H starts to drop again with increasing Ω, behaviour which would appear somewhat paradoxical to engineers (see e.g. Krieth 1968) used to associating an *enhancement* of heat transfer with the onset of turbulent flow.

The mechanisms responsible for the transitions from axisymmetric to non-axisymmetric flow and from regular non-axisymmetric flow to irregular non-axisymmetric flow are of considerable theoretical interest. It has been demonstrated fairly conclusively that the non-axisymmetric flows, with their meandering jet streams, are fully-developed 'baroclinic waves' which owe their existence to an instability of the basic axisymmetric state. The available potential energy of that state is converted into kinetic energy of the waves by a process which has been termed 'sloping convection' (see Fig. 13(b)), in which typical individual fluid elements move in trajectories that are only slightly inclined to the horizontal, at an angle which is essentially non-zero but less than the slope of isopycnic surfaces. Baroclinic waves, with a horizontal scale given by Eq. (3.11), and associated frontal systems and jet streams are characteristic features of the earth's troposphere, where they play a key role in the planetary-scale transport of heat and momentum, and it can be expected on general theoretical grounds that baroclinic waves will occur not only at other levels in the atmosphere, but also in other natural systems, such as the terrestrial oceans and the fluid regions of rapidly-rotating planets and stars, including the sun.

So far as the transition from regular baroclinic waves to irregular flow ('geostrophic turbulence') is concerned, various lines of experimental evidence and theoretical reasoning (for references see Hide and Mason 1975) point to the conclusion that irregular flow arises when the baroclinic waves are 'barotropically unstable', with the kinetic energy of the main baroclinic mode passing, through non-linear interactions, to other scales of motion. The most striking evidence comes from determinations of $m_{\max}$, the number of waves around the annulus (m) at the transition from regular to irregular waves. Reducing Θ (see Eq. (5.2)) within the regular regime tends to increase m (equal to 3 in Fig. 10(b)) and the transition to irregular flow occurs when the azimuthal wavelength $\pi(b+a)/m$, has dropped to a value $\pi(b+a)/m_{\max}$ close to 1·5 times the radial scale of the waves, according to the original annulus experiments, which covered a wide range of b/a and the other parameters (Hide 1953, 1958; see also Hide and Mason 1975). In such an anisotropic system where, owing to Coriolis forces, vertical motions are very much slower than horizontal motions and viscous effects are weak, one might expect the spirit of Fjørtoft's theorem to apply, even if not the letter (see section 2(iv) and Eq. (2.27)). By that theorem the main baroclinic wave cannot lose kinetic energy by non-linear interactions to smaller scales of motion without simultaneously losing energy to larger scales of motion, and when the azimuthal wavelength $\pi(b+a)/m$ of the main baroclinic wave is comparable with the size of the apparatus, larger scales are not available and in consequence the wave is stable (see Fig. 10(b)). Only when $\pi(b+a)/m$ is small enough, $\doteqdot 1{\cdot}5$ times the radial scale according to the experiments, are the larger scales available; non-linear interactions then produce irregular flow by continually transferring kinetic energy from the main baroclinic wave to other scales of motion.

These results concerning the nature of the irregular regime of flow have important implications for dynamical meteorology and oceanography. They also enable us to understand the principal finding of the two or three isolated laboratory investigations of thermal convection in rotating fluids undertaken prior to 1950. More than a century ago Vettin made a qualitative study of the top-surface flow in a rotating tank of fluid with a lump of ice near the centre, and thereby noticed that the axisymmetric flow patterns found at low values of Ω gave way to irregular non-axisymmetric patterns at higher values of Ω. He also drew meteorological conclusions from his laboratory work (see Fultz *et al.* 1959), but these were unpalatable to his contemporaries, presumably because such an approach to meteorological problems came too soon, at a time when the atmosphere was very incompletely observed, theoretical meteorology was isolated from other branches of science, and the subject of fluid dynamics had not yet been transformed to its present healthy state from being an activity in which (to paraphrase some recent remarks by a leading expert) 'engineers

observed effects that could not be explained and mathematicians explained effects that could not be observed.'* Nowadays, fortunately, dynamical meteorologists and oceanographers make good use of basic fluid dynamics, including the full implications of the concept of geostrophy which, as we have found in our discussion of a range of experiments with rotating fluids, plays a central role in the interpretation of a wide variety of flow phenomena. Indeed, none would now dispute that the important problems in geophysical fluid dynamics can only be tackled seriously through a combination of observational, experimental and mathematical investigations, rendered crucial by keeping basic theoretical notions in mind.

Acknowledgments

In my work over the years on rotating fluids I have been greatly helped by many colleagues and students, and I am also indebted to several agencies and institutions for financial support and other resources.

References

Acheson, D. J. and Hide R. 1973 Hydromagnetics of rotating fluids, *Reports on Progress in Physics*, 36, 159–221.

Aldridge, K. D. 1972 Axisymmetric inertial oscillations of a fluid in a rotating spherical shell, *Mathematika*, 19, 163–168.

Aldridge, K. D. and Toomre, A. 1969 Axisymmetric inertial oscillations of a fluid in a rotating spherical container, *J. Fluid Mech.*, 37, 307–323.

Batchelor, G. K. 1967 *An introduction to fluid mechanics*, Cambridge University Press.

Bennetts, D. A. and Jackson, W. D. N. 1974 Source-sink flows in a rotating annulus: a combined laboratory and numerical study, *J. Fluid Mech.*, 66, 689–705.

Benton, E. R. and Clark, A. 1974 Spin-up, *Annual Reviews of Fluid Mechanics*, 6, 257–280.

Brown, S. N. and Stewartson, K. 1976 Asymptotic methods in the theory of rotating fluids, *Proc. Symp. on Asymptotic Methods and Singular Perturbations* (New York, 1976).

Busse, F. H. and Carrigan, C. R. 1974 Convection induced by centrifugal buoyancy, *J. Fluid Mech.*, 62, 579–595.

Buzyna, G. and Veronis, G. 1971 Spin-up of a stratified fluid: theory and experiment, *Ibid.*, 50, 579–608.

Chandrasekhar, S. 1961 *Hydrodynamic and hydromagnetic stability*, Oxford University Press.

Charney, J. G. 1973 Planetary fluid dynamics. In *Dynamical meteorology* (ed. P. Morel), D. Reidel Publishing Company, Dordrecht, Holland, 97–352.

Dutton, J. A. and Johnson, D. R. 1967 The theory of available potential energy and a variational approach to atmospheric energetics, *Advances in Geophysics*, 12, 334–436.

Eckart, C. 1960 *Hydrodynamics of atmospheres and oceans*, Pergamon Press, London.

Eliassen, A. and Kleinschmidt, E. 1957 Dynamical meteorology. In *Handbuch der Physik*, 48, 1–154, Berlin, Springer-Verlag.

Fjørtoft, R. 1953 On the changes in the spectral distribution of kinetic energy for two-dimensional, non-divergent flow, *Tellus*, 5, 225–230.

Fultz, D., Long, R. R., Owens, G. V., Bohan, W., Kaylor, R. and Weil, J. 1959 Studies of thermal convection in a rotating cylinder with some implications for large-scale atmospheric motions, *Met. Mon., Amer. Met. Soc.*, 4, 1–104.

Gilman, P. A. 1975 Linear simulation of Boussinesq convection in a deep rotating spherical shell, *J. Atmos. Sci.*, 32, 1331–1352

* The systematic study of rotating fluids might have commenced in the last century had mathematicians and physicists been prepared to investigate the theoretical implications of the discovery – from analyses of meteorological data – of geostrophic motion in the atmosphere. In the event, the discovery seems to have been played down if the following words (taken from a lecture delivered in 1869) of a former president of this Society can be taken as representative of the general attitude of contemporary scientists: 'A principle has been much before the public of late which was first urged by Professor Buys-Ballot of Utrecht. It may be stated as follows: Stand with your back to the wind and the barometer will be lower on your left than on your right (in the northern hemisphere). No matter how gently the wind blows, the law is found to be true. This fact, however, is of no use to us in enabling us to judge the coming weather.'

Golitsyn, G. S. 1973 *An introduction to the dynamics of planetary atmospheres*, Hydrometeorology, Leningrad.

Greenspan, H. P. 1968 *The theory of rotating fluids*, Cambridge University Press.

Hide, R. 1953 Some experiments on thermal convection in a rotating liquid, *Quart. J. R. Met. Soc.*, 79, 161

1958 An experimental study of thermal convection in a rotating liquid, *Phil. Trans. R. Soc. Lond.*, A250, 442–478.

1967 Theory of axisymmetric thermal convection in a rotating fluid annulus, *Phys. Fluids*, 10, 56–68.

1968 On source-sink flows in a rotating fluid, *J. Fluid Mech.*, 32, 737–764.

1969 Some laboratory experiments on free thermal convection in a rotating fluid subject to a horizontal temperature gradient and their relation to the theory of the global atmospheric circulation, in *The global circulation of the atmosphere* (ed. G. A. Corby), London; Royal Meteorological Society.

1971 On geostrophic motion of a non-homogeneous fluid, *J. Fluid Mech.*, 49, 745–751.

1976 Motions in planetary atmospheres, *Quart. J. R. Met. Soc.*, 102, 1–23.

Hide, R., Ibbetson, A. and Lighthill, M. J. 1968 On slow transverse flow past obstacles in a rapidly-rotating fluid, *J. Fluid. Mech.*, 32, 251–272.

Hide, R. and Mason, P. J. 1975 Sloping convection in a rotating fluid, *Advances in Physics*, 24, 47–100.

Hide, R., and Stewartson, K. 1972 Hydromagnetic oscillations of the Earth's core, *Rev. Geophys. and Space Phys.*, 10, 579–598.

Krauss, W. 1973 *Methods and results of theoretical oceanography: I, Dynamics of the homogeneous and quasi-homogeneous ocean*, Gebrüder Borntträger, Berlin, Stuttgart.

Krieth, F. 1968 Convection heat transfer in rotating systems, *Advances in Heat Transfer*, 5, 129–251.

Lighthill, M. J. 1966 Dynamics of rotating fluids: A survey, *J. Fluid Mech.*, 26, 411–431.

Lilly, D. K. 1973 Lectures on sub-synoptic scales af motions and two-dimensional turbulence. In *Dynamical meteorology* (ed. P. Morel) D. Reidel Publishing Company, Dordrecht, Holland, 353–418.

Lineykin, P. S. 1974 Theory of the main thermocline (a review), *Akad. Nauk. Okeanograf. Kom., Okeanologiya*, 14, 965–981.

Lorenz, E. N. 1967 *The nature and theory of the general circulation of the atmosphere*. World Meteorological Organization Publication No. 218.

Mason, P. J. 1976 Forces on spheres moving horizontally in a rotating stratified fluid, *Geophys. Fluid Dyn.*, 7.

McEwan, A. D. 1976 Angular momentum diffusion and the initiation of cyclones, *Nature*, 260, 126–128.

Monin, A. S. 1972 *Weather forecasting as a problem in physics*, M.I.T. Press, Cambridge, Mass.

Obukhov, A. M. 1974 Global invariants of atmospheric motions pp. 106–112 in *Physical and dynamical climatology*, World Meterological Organization Monograph No. 347, Hydrometerology, Leningrad.

Pedlosky, J. 1971 Geophysical fluid dynamics, *Lectures in Applied Mathematics*, 13, 1–60.

Phillips, N. A. 1963 Geostrophic motion, *Rev. Geophys*, 1, 123–173.

Platzman, G. W. 1968 The Rossby wave, *Quart. J. R. Met. Soc.*, 94, 225–248.

Prandtl, L. 1952 *Essentials of fluid dynamics*, London; Blackie and Sons.

Proudman, J. 1916 On the motions of solids in a liquid possessing vorticity, *Proc. R. Soc. Lond.*, A92, 408–424.

Quinet, A. 1974 A numerical study of vacillation, *Advances in Geophysics*, 17, 101–186.

Rhines, P. B. 1976 The dynamics of unsteady currents, In *The sea*, Vol. VI, pp. 189–318. E. Goldberg, ed. John Wiley and Sons, New York.

Spiegel, E. A.	1972	Convection in stars. II. Special effects, *Ann. Rev. Astronomy Astrophys*, 10, 261–304.
Stern, M. E.	1975	*Ocean circulation physics*, Vol. 19. International Geophysics Series, Academic Press.
Stommel, H.	1965	*The Gulf Stream*, University of California Press.
Taylor, G. I.	1917	Motion of solids in fluids when the flow is not irrotational, *Proc. R. Soc.*, A93, 99–113.
	1923	Experiments on the motion of solid bodies in rotating fluids, *Proc. R. Soc. Lond.*, A104, 213–218.
	1974	The interaction between experiment and theory in fluid mechanics, *Ann. Rev. Fluid Dyn.*, 6, 1–16.
Thompson, P. D.	1961	*Numerical weather analysis and prediction*, MacMillan Co., New York.
Turner, J. S.	1973	*Buoyancy effects in fluids*, Cambridge University Press.
Van Mieghem, J.	1973	*Atmospheric energetics*, Clarendon Press, Oxford.
Veronis, G.	1973	Large scale ocean circulation, *Advances in Applied Mechanics*, 13, 1–92. (ed. C. S. Yih, Academic Press, New York and London.)

NOTE ADDED IN PROOF. According to Dr A. E. Gill (private communication), one example of Kelvin waves (see page 10 above) in the troposphere are the 'coastal laws' that propagate around the southern end of the African continent at all times of the year.